Brain metastases from different primary carcinomas

Zhang, Hao; Zhang, G.; Oudkerk, M.

IMPORTANT NOTE: You are advised to consult the publisher's version (publisher's PDF) if you wish to cite from it. Please check the document version below.

Document Version
Publisher's PDF, also known as Version of record

[Link to publication in University of Groningen/UMCG research database](#)

Brain Metastases from Different Primary Carcinomas: an Evaluation of DSC MRI Measurements

H. ZHANG[1], G. ZHANG[1], M. OUDKERK[2]

[1] Department of Radiology, Shanghai Jiaotong University Affiliated First People's Hospital; Shanghai, China
[2] Department of Radiology, University Medical Center Groningen, University of Groningen; Groningen, The Netherlands

SUMMARY – *This study evaluated the roles of different dynamic susceptibility contrast magnetic imaging (DSC MRI) measurements in discriminating between brain metastases derived from four common primary carcinomas. Thirty-seven patients with brain metastases were enrolled. Relative cerebral blood volume (rCBV), cerebral blood flow (rCBF) and relative mean transit time (rMTT) in both tumor and peritumoral edema were measured. Metastases were grouped by their primary tumor (lung, gastrointestinal, breast and renal cell carcinoma). DSC MRI measurements were compared between groups. Mean rCBV, rCBF, rMTT in tumor and peritumoral edema of all brain metastases (n=37) were 2.79 ± 1.73, 2.56 ± 2.11, 1.21 ± 0.48 and 1.05 ± 0.53, 0.86 ± 0.40, 1.99 ± 0.41, respectively. The tumoral rCBV (5.26 ± 1.89) and rCBF (5.32 ± 3.28) of renal metastases were greater than those of the other three metastases (P<0.05). The tumoral rMTT (1.58 ± 0.77) of breast metastases was statistically greater than that (0.96 ± 0.31) of gastrointestinal metastases (P=0.013). No statistical difference was found between peritumoral rCBV, rCBF and rMTT (P>0.05). Evaluating various DSC MRI measurements can provide complementary hemodynamic information on brain metastases. The tumoral rCBV, rCBF and likely rMTT can help discriminate between brain metastases originating from different primary carcinomas. The peritumoral DSC MRI measurements had limited value in discriminating between brain metastases.*

Introduction

Brain metastases are the most common tumors of the central nervous system[1]. The exact incidence of brain metastases is unknown. Autopsy and clinical studies suggest that the incidence of brain metastases is much higher than epidemiological studies have revealed so far[1]. Schouten et al. studied the incidence of brain metastases in a cohort of USA patients with carcinoma of the breast, colon, kidney, lung and malignant melanoma[2]. They found that the cumulative incidence of brain metastases after five years was highest in patients with lung carcinoma (16.3%) followed by patients with renal carcinoma (9.8%), breast carcinoma (7.4%), malignant melanoma (5.0%) and colorectal carcinoma (1.2%).

Most cases of brain metastases present with multiple intracranial lesions, and a known history of primary malignancy elsewhere in the body can be diagnosed with sufficient accuracy by using conventional MR imaging alone. Nevertheless, differentiation between a large solitary metastasis and primary brain tumor can be difficult in some cases using the morphological features shown on routine MR images. It is also difficult on morphological grounds to predict the primary tumor of a metastasis, for the purpose of selecting further investigations.

Perfusion MR imaging can provide vascular information on brain tumors. Multiple studies have shown that perfusion MR techniques can help preoperative assessment of tumor histology, guide stereotactic biopsy and monitor treatment effects. However, brain metastases involved in perfusion MRI studies[3-5] were

mostly evaluated only their CBV measurement without considering their primary tumors and histology. Brain metastases derived from different primary tumors may demonstrate different perfusion characteristics. Kremer et al. studied a limited number of brain metastases using a DSC MRI technique and illustrated that the rCBV of melanoma and renal metastases were significantly higher than those of lung carcinoma metastases [6]. To our knowledge, no publications evaluated other dynamic susceptibility contrast magnetic imaging (DSC MRI) measurement such as relative cerebral blood flow (rCBF) and relative mean transit time (rMTT) of brain metastases of different origin. Discrimination of brain metastases derived from different primary tumors can help to distinguish their histology which is of particular importance when considering whole brain radiation therapy (WBRT) for patients with radio-resistant tumors who could benefit from the progress of newly developing target therapies for brain metastases [7,8]. A lack of thorough DSC MRI information of brain metastases motivated this research. The purpose of this study was to evaluate the characteristics of different DSC MRI measurements of brain metastases from four common primary carcinomas, hoping to provide helpful imaging information for the differential diagnosis between brain metastases.

Materials and Methods

Patients

Thirty-seven patients (20 men; patient age 32-78 years; mean age 53 years) with brain metastases (15 from lung carcinoma; nine from gastrointestinal carcinoma; eight from breast carcinoma and five from renal cell carcinoma) were enrolled in this retrospective study. Nineteen patients had a single cerebral metastasis, the other 18 patients had multiple cerebral metastases. All patients underwent both conventional and perfusion-weighted MR imaging before treatment. Furthermore, all of them underwent surgical resection or stereotactic brain biopsy within one month after MR scanning. The results were confirmed pathologically and supported by follow-up clinical data with respect to the primary tumors. This study was approved by local ethical committee, patients' written informed consent was obtained for MRI examinations.

MRI protocol

MR examinations were performed with a 1.5T clinical system (Signa, GE Medical Systems, Milwaukee, WI, USA). Pre-enhancement sagittal and axial T1-weighted SE (TR/TE=440/14 ms, matrix, 256*256; section thickness, 6 mm; field of view 22 cm), pre-enhancement axial fluid attenuated inversion recovery (FLAIR) sequences (TR/TE=8002/126 ms, TI=2000 ms) were performed ten minutes before DSC MR imaging. Then 15 ml contrast agent (Gd-DTPA, 0.1 mmol/kg, Omniscan, GE Medical Systems, Milwaukee, WI, USA) was administered intravenously with a power injector (Medrad, Indianola, PA, USA) at a rate of 4 ml/s, followed by a 20 ml saline flush at the same rate. Five seconds after the beginning of injection DSC MRI was performed by using a multi-slice gradient echo-planar sequence with the following parameters: 1800/40/1(TR/TE/excitations); flip angle, 60°; bandwidth, 62.75; matrix, 128*128; number of sections, ten; section thickness, 6 mm with spacing of 0 mm; field of view, 22 cm. Total scan time was one minute 38 seconds. A series of 50 dynamic acquisitions was obtained for each section. Lastly, a post-enhancement axial T1-weighted SE sequence was performed with the same slice selection and thickness as the DSC sequence.

Data Analysis

Image analysis was performed Functool software (ADW 4.0 workstation, GE Medical Systems, Milwaukee, WI, USA). A dynamic perfusion technique with a contrast medium demonstrates cerebral hemodynamics by analyzing changes in the signal intensities after administration of contrast material. During the first pass of the contrast agent, which was administered rapidly, both T2* relaxation time and its equivalent T2* signal intensity decreased. The change in relaxation rate ($\Delta R2^*$) could be calculated on the basis of signal intensity by means of the following equation: $\Delta R2^*(t)=\{Kln (S(t)/S(0))\}/TE$. In this equation, TE=echo time, S(0)=baseline signal intensity and S(t)= signal intensity at a specific time. $\Delta R2^*$ is proportional to the concentration of contrast agent in tissue and this calculation allows conversion of a time-signal intensity curve into a time-concentration curve. CBV is proportional to the area under the time-concentration curve. The measurement of CBV is subject to errors caused by recirculating contrast in the vessels and the extravascular leakage of contrast agents in some

brain tumors with severe blood-brain barrier disruption. A gamma-variate curve-fitting technique is used to eliminate the contamination of the first pass bolus due to contrast agent recirculation and extravascular leakage. Furthermore, the contrast agents administered just before DSC MR imaging for post-enhancement T1-weighted imaging can mitigate some of the T1-shortening effect and thus reduce the error caused by contrast leakage. rCBV maps were generated as color scale images by numerical integration of the area under the fitted curve on a pixel-by-pixel basis. Once the time-signal intensity curve has been calculated for each region of interest (ROI), the value of the width of the curve when it reaches one half of its maximum value (full width-half maximum) is proportional to the rMTT, whereas the maximum slope of the decrease in signal intensity after contrast arrival is proportional to rCBF. The perfusion parameters derived from this system are relative (rCBV, rCBF and rMTT) measurements. In this study, the rCBV, rCBF and rMTT values were further normalized by dividing lesional values into the values obtained from the contralateral healthy white matter.

To target regions of maximal abnormality, three to five circular ROIs (depending on the size of the lesion), at least 20 mm^2 each, were placed at the solid part in the tumor and peritumoral edema by referring to FLAIR, post-contrast TWI images and functional color maps (Figures 1 and 2). The maximal rCBV, rCBF and rMTT of tumor and peritumoral edema were recorded. For patients with multiple metastases, the largest supratentorial lesion was selected for evaluation. ROI placement should avoid arterial or venous structures in tumor and peritumoral edema. The peritumoral edema was defined as a high signal area on FLAIR images within a 1 cm distance from the outer enhancing tumor margin on post-enhanced T1-weighted images [3]. Another ROI was placed at the contralateral unaffected white matter of the same section.

Metastases were grouped by their primary tumors (lung, gastrointestinal, breast and renal cell carcinomas). Statistical analysis was performed with commercially available statistical software (SPSS, version 14.0 for Windows; SPSS, Chicago, IL, USA). The rCBV, rCBF and rMTT of each group were expressed as mean ± standard deviation. The differences between groups were first compared by using one-way ANOVA. Fisher's least significant difference (LSD) tests were then performed for necessary multiple comparisons of each pair of metastases. A P value < 0.05 indicated a statistically significant difference.

Results

Examples of brain metastases are given in Figures 1 and 2. Most metastases enhanced unevenly on post-enhancement T1W images with or without hemorrhage, cystic or necrotic areas in tumor and had moderate or severe peritumoral edema. On conventional MR images, no specific morphological features could be used to identify the primary tumors of brain metastases. Among 19 single metastases, ten cases with a clear clinical history of primary malignant carcinomas were diagnosed correctly as metastases using conventional MRI sequences and the other nine cases (47.3%) with no recorded history of primary malignant tumor in other parts of the body were diagnosed as possible gliomas or metastases preoperatively.

The mean normalized rCBV, rCBF, rMTT values in tumor (T rCBV, T rCBF, T rMTT) and in peritumoral edema (P rCBV, P rCBF, P rMTT) of brain metastases in all (n=37) were 2.79 ± 1.73, 2.56 ± 2.11, 1.21 ± 0.48 and 1.05 ± 0.53, 0.86 ± 0.40, 1.99 ± 0.41 respectively. The perfusion measurement values of each kind of brain metastases and one-way ANOVA results are summarized in Table 1. The T rCBV and T rCBF between groups were statistically different (P<0.05). No statistical difference was noted between T rMTT, P rCBV, P rCBF and P rMTT values of the four groups (P>0.05). Multiple comparisons between each two groups demonstrated that the T rCBV (5.26 ± 1.89) and T rCBF (5.32 ± 3.28) of renal metastases were maximum and both statistically greater (P<0.05) than the corresponding measurements of other groups (Table 2). The T rMTT (1.58 ± 0.77) of breast metastases was statistically greater than that (0.96 ±0.31) of gastrointestinal metastases (P=0.013) (Table 3). No statistical difference was found between P rCBV, P rCBF and P rMTT values of each two groups (P>0.05).

Discussion

To become a central nervous system metastasis, cancer cells which ten genetically to metastasize must undergo a complex series of steps. The changes in microcirculation of both tumor

A

B

C

D

E
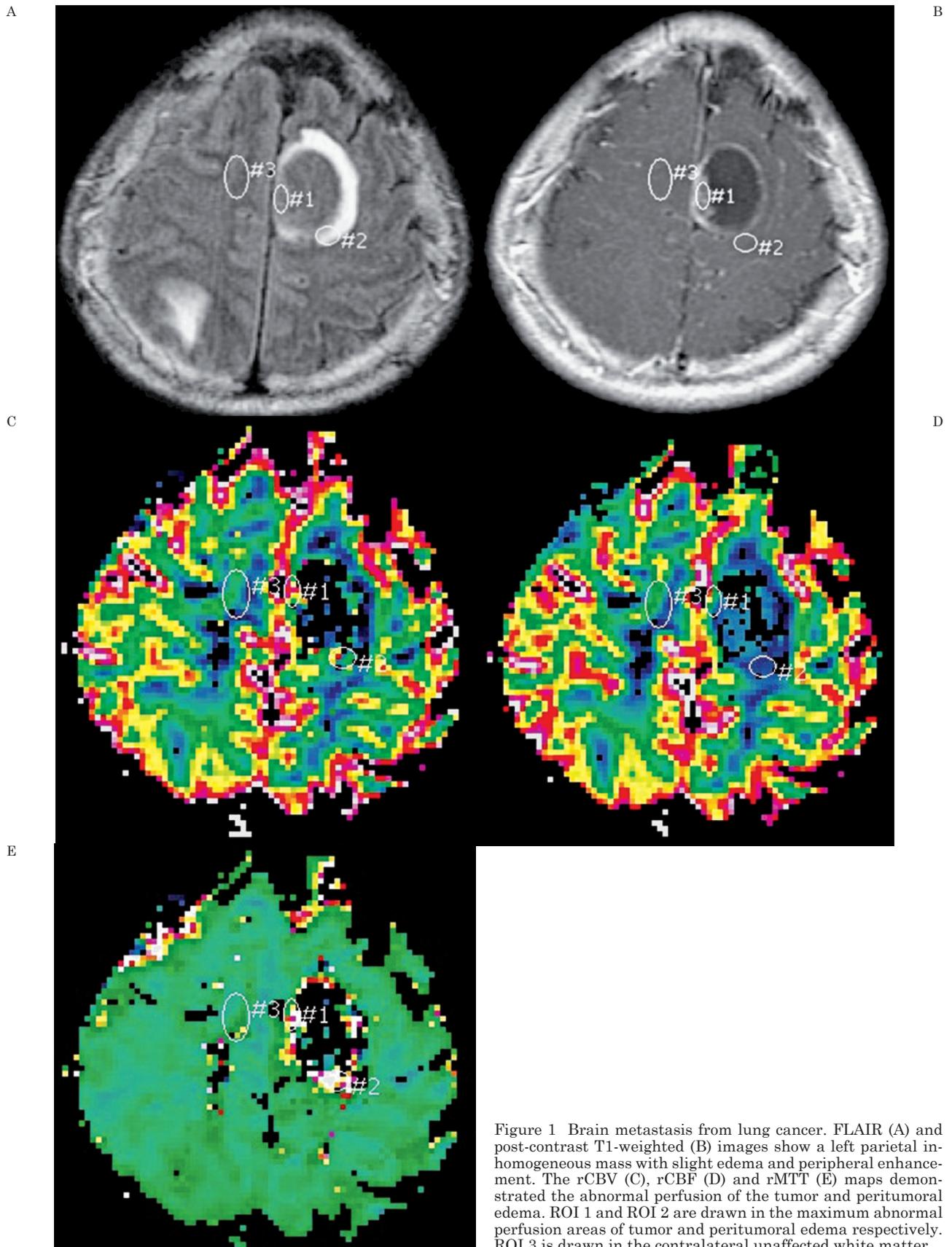
Figure 1 Brain metastasis from lung cancer. FLAIR (A) and post-contrast T1-weighted (B) images show a left parietal inhomogeneous mass with slight edema and peripheral enhancement. The rCBV (C), rCBF (D) and rMTT (E) maps demonstrated the abnormal perfusion of the tumor and peritumoral edema. ROI 1 and ROI 2 are drawn in the maximum abnormal perfusion areas of tumor and peritumoral edema respectively. ROI 3 is drawn in the contralateral unaffected white matter.

Table 1 DSC MRI values of brain metastases from different primary carcinomas.

Perfusion parameters	Lung cancer (n=15)	Gastrointestinal carcinoma (n=9)	Breast cancer (n=8)	Renal cell carcinoma (n=5)	P value
T rCBV	2.42 ± 1.57	1.83 ± 0.82	2.75 ± 0.92	5.26 ± 1.89	0.001*
P rCBV	1.07 ± 0.48	1.09 ± 0.47	0.86 ± 0.47	1.18 ± 0.84	0.788
T rCBF	2.34 ± 1.80	1.56 ± 0.71	2.12 ± 0.82	5.32 ± 3.28	0.006*
P rCBF	0.96 ± 0.44	0.90 ± 0.31	0.69 ± 0.29	0.83 ± 0.63	0.676
T rMTT	1.12 ± 0.31	0.96 ± 0.31	1.58 ± 0.77	1.40 ± 0.25	0.062
P rMTT	1.11 ± 0.19	1.05 ± 0.30	1.37 ± 0.80	1.33 ± 0.16	0.412

*, one way ANOVA, P value <0.05 indicates a statistically significant difference.
Note: T rCBV, T rCBF, T rMTT represent relative cerebral blood volume, cerebral blood flow, mean transit time in tumor and P rCBV, P rCBF, P rMTT are the corresponding measurments in peritumoral edema respectively. All values are normalized by dividing lesional values into the values obtained from the contralateral healthy white matter.

Table 2 T rCBV/ T rCBF difference between each two groups of brain metastases.

	Lung cancer	Gastrointestinal carcinoma	Renal cell carcinoma
Breast cancer	P = 0.633 / 0.818	P = 0.200 / 0.547	P = 0.005* / 0.006*
Lung cancer		P = 0.360 / 0.355	P = 0.001* / 0.005*
Gastrointestinal carcinoma			P = 0.000* / 0.001*

*: Least significant difference (LSD) test, the mean difference is significant at the 0.05 level. P values for relative cerebral blood volume (T rCBV) / relative cerebral blood flow (T rCBF) in tumor, respectively.

Table 3 T rMTT difference between each two groups of brain metastases.

	Lung cancer	Gastrointestinal carcinoma	Renal cell carcinoma
Breast cancer	P = 0.060	P = 0.013*	P = 0.495
Lung cancer		P = 0.445	P = 0.279
Gastrointestinal carcinoma			P = 0.090

*: Least significant difference (LSD) test, the mean difference is significant at the 0.05 level. P values for relative mean transit time in tumor (T rMTT).

and peritumoral brain tissue play an important role in this process [1]. Previous pathophysiological findings [9,10] demonstrated that the capillary endothelium of metastatic brain tumors showed increased permeability and was similar to capillaries from the tissue of origin. Oncology studies demonstrated that the response rate of brain metastases to chemotherapy was similar to the response rate of the primary tumors and extracranial metastases, some tumor types were more chemosensitive (small cell lung carcinoma, breast carcinoma, germ cell tumors) [11]. On the other hand, patients with brain metastases derived from melanoma, renal cell carcinoma, or sarcoma are more radioresistant and may be of less benefit from whole brain radiation therapy than other metastases [7]. Furthermore, as novel therapies such as antiangiogenic and target management for patients with brain metastases are being developed, the role of imaging has begun to shift to provide information on tumor physiology as well as anatomy [8,12]. Evaluating the vascular characteristics of brain metastases from different primary carcinomas may help make a more accurate diagnosis and a better choice of therapeutic management for brain metastases.

MR imaging, specifically contrast-enhanced T1-weighted MR imaging, has proven to be the most sensitive diagnostic modality for lesion detection and delineation of the morphological features of brain metastases [13]. However, the anatomic information offered by conventional MRI is often not enough to reach a specific
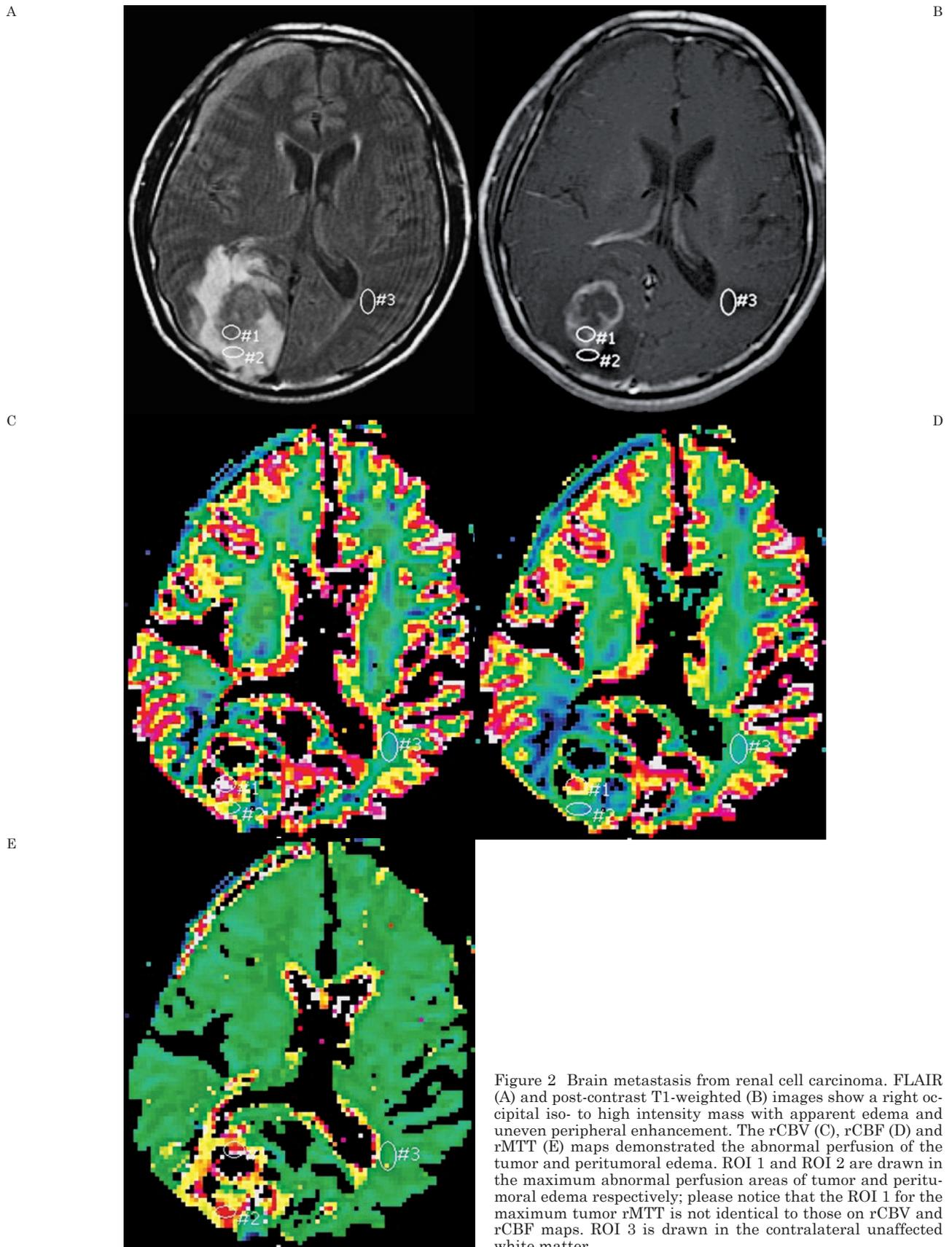
Figure 2   Brain metastasis from renal cell carcinoma. FLAIR (A) and post-contrast T1-weighted (B) images show a right occipital iso- to high intensity mass with apparent edema and uneven peripheral enhancement. The rCBV (C), rCBF (D) and rMTT (E) maps demonstrated the abnormal perfusion of the tumor and peritumoral edema. ROI 1 and ROI 2 are drawn in the maximum abnormal perfusion areas of tumor and peritumoral edema respectively; please notice that the ROI 1 for the maximum tumor rMTT is not identical to those on rCBV and rCBF maps. ROI 3 is drawn in the contralateral unaffected white matter.

diagnosis and come to a justifiable treatment decision: additional diagnostic and clinical information is necessary [14-16]. The enhancing portion of brain metastases on post-contrast T1WI is mainly due to the breakdown or lack of the blood-brain barrier and the leakage of contrast agent from capillary to extracellular space rather than to tumor vessel proliferation. Thus, the enhancement pattern does not give precise information on tumor angiogenesis at the capillary level [17,18]. This explains why the morphological features of metastases such as uneven enhancement, hemorrhage, cystic or necrotic areas in tumor parenchyma and the peritumoral edema on conventional MR images give no reliable clues for the location of the primary tumors. In case of single brain metastases, especially without a known primary tumor, it is difficult to differentiate metastasis from primary malignant brain tumors or nonneoplastic conditions with conventional MRI [11]. These correspond to our results which demonstrated that no specific morphological features on conventional MRI images could be used to identify the primary tumors of brain metastases and among 19 patients with single metastases, nine cases (47.3%) could not be definitely differentiated from gliomas.

DSC MR imaging can evaluate tumor vasculature by measuring the degree of tumor angiogenesis and capillary permeability, which are important factors for both growth and prognosis of brain tumors [1,11]. DSC MRI studies demonstrated that both neovascularization and increased vascular permeability can result in an increased tumoral blood volume (CBV) in gliomas [19-21]. DSC MRI studies associated with brain metastases were mainly focused on its application in the differentiation of single brain metastases from primary brain tumors, especially high grade gliomas [3-5,22,23]. However, results seemed controversial or mixed. Law et al. and Chiang et al. showed that the rCBVs in the peritumoral regions of high-grade gliomas and metastases were statistically different while no statistically significant difference was noted between the intratumoral rCBV values of theses two entities [3,4]. Another study by Bulakbasi et al. found that both tumoral rCBVs and rCBVs in the peritumoral region were statistically different between high-grade gliomas and metastases [5]. However, two recent studies [22,23] by Fayed et al. illustrated that rCBVs in the peritumoral region and lesion center did not yield any statistically significant differences between gliomas and brain metastases. They

concluded that perfusion MRI has not demonstrated predictive power to distinguish brain tumors. Besides the controversial results, the rCBV values of brain metastases varied in a broad range in these studies, especially those of intratumoral rCBVs. Regardless of the data processing methods and the definite values shown in these papers, the intratumoral rCBVs of brain metastases varied from greater than [3], to similar to [22,23] and to less than [5] those of high-grade gliomas. After reviewing the patients' data in these studies, we noted that greater rCBVs of brain metastases occurred when renal and melanoma metastases were included [3] and otherwise, the results were inverted [5]. Our results demonstrated that T rCBV of renal metastases was significantly greater than those of other metastases ($P<0.05$) and there was no statistical difference between T rCBVs of lung, breast and gastrointestinal carcinoma metastases ($P>0.05$). Another study by Kremer et al. also showed that the mean rCBV of melanoma metastases (5.35 ± 2.32) and of renal carcinoma metastases (8.17 ± 2.39) were significantly greater than those of high-grade astrocytomas (2.61 ± 1.17) ($P=0.002$ and <0.001, respectively) and of lung carcinoma metastases (2.94 ± 0.86) ($P=0.003$ and 0.002) [6]. There was no statistically significant difference between the mean rCBV of lung metastases and of high-grade astrocytomas ($P=0.59$). The elevated rCBV of renal and melanoma metastases suggested that they were hypervascular lesions and had rich vascularity similar to their primary tumors [24]. These may partly explain the controversial results mentioned above. Based on previous studies and ours, we concluded that different enrollments of patient with brain metastases can lead to different results in DSC MRI studies. Evaluating brain metastases separately by their primary tumors may provide more accurate information on their vascularity and might be more helpful in differential diagnosis of brain tumors.

Most DSC MRI studies evaluated only the regional blood volume of brain metastases [3-5,22,23]. Other perfusion measurements such as the relative cerebral blood flow (rCBF) and the relative mean transit time (rMTT) of brain metastases have seldom been evaluated. Studies of other imaging techniques like single-photon emission computed tomography (SPECT) and positron emission tomography (PET) demonstrated that evaluating the CBF of brain metastases was useful in tumor detection but did not discriminate the lesions from different

primary brain tumors [25-27]. Arterial spin-labeling (ASL) perfusion MRI studies showed that evaluating the CBF changes of brain metastases can help distinguish glioblastomas from metastases and predict treatment outcome before and after stereotactic radiosurgery [28,29]. By comparing results derived from DSC and ASL MRI, Warmuth et al. found a close correlation between these two methods in the determination of blood flow in brain tumors [30].

The rCBF can be affected by both the density and the velocity changes in tumor capillaries. The T rCBF (2.56 ± 2.11) of brain metastases in all our results corresponded with the mild to moderate proliferation and increased blood flow in brain metastases at microvascular level [31]. The T rMTT (1.21 ± 0.48) of brain metastases in our results reflected the prolonged mean transit time of contrast agents in tumors and might be attributed to the low and heterogeneous microvascular red blood cell velocity, elevated hematocrit and increased geometric resistance of the tumor microvasculature [32,33]. Usually, rCBF and rCBV measurements are tightly coupled [13]. Similar to T rCBV, the T rCBF of renal metastases was significantly greater than those of other brain metastases in this study ($P<0.05$). Our results suggested that rCBF derived from DSC MRI can also help discriminate brain metastases originated from these four primary carcinomas. In our results, while no statistical difference between T rMTTs of the four metastases groups ($P>0.05$) was found by one-way ANOVA tests, Fisher's least significant difference (LSD) tests showed that the T rMTT (1.58 ± 0.77) of breast metastases was statistically greater than that (0.96 ± 0.31) of gastrointestinal metastases ($P=0.013$). From a statistical standpoint, this inconsistent result means that the statistical power of comparison should be questioned and if the sample size is increased, the result could change. Hence, further DSC MRI studies including more patients are needed to verify this difference between breast and gastrointestinal metastases.

In our results, the P rCBV, P rCBF and P rMTT showed no statistically significant differences between groups ($P>0.05$). The P rCBV, P rCBF and P rMTT of all metastatic tumors in our study were 1.05 ± 0.53, 0.86 ± 0.40 and

1.99 ± 0.41 respectively. Histopathological studies deduced the slightly increased regional blood volume in peritumoral edema from mild to glomeruloid microvascular proliferation occurred in peritumoral neuroglial tissue of cerebral metastases. Consequently, the accumulation of peritumoral edema fluid did not cause microcirculatory compression as long as intracranial pressure was not critically increased. The reduction of regional blood flow might contribute to the increase in tissue water content in the peritumoral white matter and the volumetric expansion of edematous tissue, while the prolonged mean transit time was supposed to be mainly due to the increased vascular resistance caused by the mass effects of extracellular fluid accumulation [31,34,35]. Our results suggest that no unique vascular characteristics in peritumoral edema of different metastases could be demonstrated by DSC MRI and the usefulness of peritumoral DSC MRI measurements for discrimination between brain metastases derived from different primary carcinomas is limited. However, like previous DSC MRI studies [3-5] have demonstrated, evaluating these hemodynamic features in the peritumoral edema of brain metastases allowed differentiation of them from primary brain tumors with no need for considering their histology.

In conclusion, no specific morphological features on conventional MRI images could be used to identify the primary tumors of brain metastases. Evaluating various DSC MRI measurements can provide complementary hemodynamic information of brain metastases at the microvascular level. The maximum rCBV, rCBF and likely rMTT measured in tumor parenchyma can help the discrimination between brain metastases originated from different primary carcinomas. Specifically in this study, the T rCBV and T rCBF were effective in the differentiation of renal metastasis from lung, breast and gastrointestinal metastases; the T rMTT was possibly useful in the differentiation between breast and gastrointestinal metastases. The peritumoral DSC MRI measurements disclosed limited value in discrimination between brain metastases. Further DSC MRI studies including more patients for individual metastatic groups are needed to verify our results.

References

1 Gavrilovic IT, Posner JB. Brain metastases: epidemiology and pathophysiology. J Neurooncol. 2005; 75: 5-14.
2 Schouten LJ, Rutten J, Huveneers HA, et al. Incidence of brain metastases in a cohort of patients with carcinoma of the breast, colon, kidney, and lung and melanoma. Cancer. 2002; 94: 2698-2705.
3 Law M, Cha S, Knopp EA, et al. High-grade gliomas and solitary metastases: differentiation by using perfusion and proton spectroscopic MR imaging. Radiology. 2002; 222: 715-721.
4 Chiang IC, Kuo YT, Lu CY, et al. Distinction between high-grade gliomas and solitary metastases using peritumoral 3-T magnetic resonance spectroscopy, diffusion, and perfusion imagings. Neuroradiology. 2004; 46: 619-627.
5 Bulakbasi N, Kocaoglu M, Farzaliyev A, et al. Assessment of diagnostic accuracy of perfusion MR imaging in primary and metastatic solitary malignant brain tumors. Am J Neuroradiol. 2005; 26: 2187-2199.
6 Kremer S, Grand S, Berger F, et al. Dynamic contrast-enhanced MRI: differentiating melanoma and renal carcinoma metastases from high-grade astrocytomas and other metastases. Neuroradiology. 2003; 45: 44-49.
7 Peacock KH, Lesser GJ. Current therapeutic approaches in patients with brain metastases. Curr Treat Opt Oncol. 2006; 7: 479-489.
8 Eichler AF, Loeffler JS. Multidisciplinary management of brain metastases. Oncologist. 2007; 12: 884-898.
9 Van den Hauwe L, Parizel PM, Martin JJ, et al. Postmortem MRI of the brain with neuropathological correlation. Neuroradiology 1995; 37: 343-349.
10 Zhang M, Olsson Y. Hematogenous metastases of the human brain: characteristics of peritumoral brain changes - a review. J Neurooncol. 1997; 35: 81-89.
11 Soffietti R, Ruda R, Mutani R. Management of brain metastases. J Neurol. 2002; 249: 1357-1369.
12 Covarrubias DJ, Rosen BR and Lev MH. Dynamic magnetic resonance perfusion imaging of brain tumors. Oncologist. 2004; 9: 528-537.
13 Schellinger PD, Meinck HM, Thron A. Diagnostic accuracy of MRI compared to CT in patients with brain metastases. J Neurooncol. 1999; 44: 275-281.
14 Essig M, Knopp MV, Schoenberg SO, et al. Cerebral gliomas and metastases: assessment with contrast-enhanced fast fluid attenuated inversion-recovery MR imaging. Radiology. 1999; 210: 551-557.
15 Hawighorst H, Essig M, Debus J, et al. Serial MR imaging of intracranial metastases after radiosurgery. Magn Reson Imag. 1997; 15: 1121-1132.
16 Peterson AM, Meltzer CC, Evanson EJ, et al. MR imaging response of brain metastases after gamma knife streotactic radiosurgery. Radiology. 1999; 211: 807-814.
17 Huber PE, Hawighorst H, Fuss M, et al. Transient enlargement of contrast uptake on MRI after linear accelerator (LINAC) stereotactic radiosurgery for brain metastases. Int J Radiat Oncol Biol Phys. 2001; 49: 1339-1349.
18 McKnight TR, von dem Bussche MH, Vigneron DB. Histopathological validation of a three-dimensional magnetic resonance spectroscopy index as a predictor of tumor presence. J Neurosurg. 2002; 97: 794-802.
19 Cha S, Johnson G, Wadghiri YZ, et al. Dynamic, contrast-enhanced perfusion MRI in mouse gliomas: correlation with histopathology. Magn Reson Med. 2003; 49: 848-855.
20 Law M, Yang S, Babb JS, et al. Comparison of cerebral blood volume and vascular permeability from dynamic susceptibility contrast-enhanced perfusion MR imaging with glioma grade. Am J Neuroradiol. 2004; 25: 746-755.
21 Aronen HJ, Gazit IE, Louis DN, et al. Cerebral blood volume maps of gliomas: comparison with tumor grade and histologic findings. Radiology. 1994; 191: 41-51.
22 Fayed N, Modrego PJ. The contribution of magnetic resonance spectroscopy and echoplanar perfusion-weighted MRI in the initial assessment of brain tumours. J Neurooncol. 2005; 72: 261-265.
23 Fayed N, Dávila J, Medrano J, et al. Malignancy assessment of brain tumours with magnetic resonance spectroscopy and dynamic susceptibility contrast MRI. Eur J Radiol. 2008; 67: 427-433.
24 Rosen MA and Schnall MD. Dynamic contrast-enhanced magnetic resonance imaging for assessing tumor vascularity and vascular effects of targeted therapies in renal cell carcinoma. Clin Cancer Res. 2007; 13: 770-776.
25 Katano H, Karasawa K, Sugiyama N, et al. Comparison of thallium-201 uptake and retention indices for evaluation of brain lesions with SPECT. J Clin Neurosci. 2002; 9: 653-658.
26 Wong TZ, van der Westhuizen GJ, Coleman R. Positron emission tomography imaging of brain tumors. Neuroimag Clin N Am. 2002; 12: 615-626.
27 Lassen U, Andersen P, Daugaard G, et al. Metabolic and hemodynamic evaluation of brain metastases from small cell lung cancer with positron emission tomography. Clin Cancer Res. 1998; 4: 2591-2597.
28 Weber MA, Zoubaa S, Schlieter M, et al. Diagnostic performance of spectroscopic and perfusion MRI for distinction of brain tumors. Neurology. 2006; 66: 1899-1906.
29 Weber MA, Thilmann C, Lichy MP, et al. Assessment of irradiated brain metastases by means of arterial spin-labeling and dynamic susceptibility-weighted contrast-enhanced perfusion MRI: initial results. Invest Radiol. 2004; 39: 277-87.
30 Warmuth C, Gunther M, Zimmer C. Quantification of blood flow in brain tumors: comparison of arterial spin labeling and dynamic susceptibility-weighted contrast-enhanced MR imaging. Radiology. 2003; 228: 523-532.
31 Wesseling P, Vandersteenhoven JJ, Downey BT, et al. Cellular components of microvascular proliferation in human glial and metastatic brain neoplasms. Acta Neuropathol. 1993; 85: 508-514.
32 Vajkoczy P, Schilling L, Ullrich A, et al. Characterization of angiogenesis and microcirculation of high-grade glioma: an intravital multifluorescence microscopic approach in the athymic nude mouse. J Cereb Blood Flow Metab. 1998; 18: 510-520.
33 Baish JW, Gazit Y, Berk DA, et al. Role of tumor vascular architecture in nutrient and drug delivery: an invasion percolation-based network model. Microvasc Res. 1996; 51: 327-346.
34 Hossmann K-A. The pathophysiology of experimental brain edema. Neurosurg Rev. 1989; 12: 263-280.
35 Roy S, Sarkar C. Ultrastructural study of micro-blood vessels in human brain tumors and peritumoral tissue. J Neurooncol. 1989; 7: 283-292.

Hao Zhang, MD
Department of Radiology
Shanghai Jiaotong University
affiliated First People's Hospital
100 Haining Road
Shanghai 200080, China
Tel.: +31 50 36 11098
Fax: +31 50 36 191 68
E-mail: zhanghao021@gmail.com